JOURNAL OF BACTERIOLOGY, Jan. 2008, p. 515–526 Vol. 190, No. 2
0021-9193/08/$08.00+0 doi:10.1128/JB.01219-07

Characterization of Integrative and Conjugative Element ICE*Kp1*-Associated Genomic Heterogeneity in a *Klebsiella pneumoniae* Strain Isolated from a Primary Liver Abscess[▽]

Tzu-Lung Lin,[1] Cha-Ze Lee,[2] Pei-Fang Hsieh,[1] Shih-Feng Tsai,[3,4] and Jin-Town Wang[1,2]*

Department of Microbiology, National Taiwan University College of Medicine, Taipei,[1] Department of Internal Medicine, National Taiwan University Hospital, Taipei,[2] Faculty of Life Sciences and Institute of Genetics, National Yang-Ming University, Taipei,[3] and Division of Molecular and Genomic Medicine, National Health Research Institute, Zhunan, Miaoli,[4] Taiwan

Received 29 July 2007/Accepted 25 October 2007

Genomic heterogeneity has been shown to be associated with *Klebsiella pneumoniae* strains causing pyogenic liver abscesses (PLA) and metastatic infections. In order to explore the mechanism responsible for genomic heterogeneity in *K. pneumoniae*, we compared the complete genomic sequences of strains NTUH-K2044 and MGH78578. An ~76-kbp DNA fragment located adjacent to an asparagine (*asn*) tRNA gene was present in NTUH-K2044 but not in MGH78578. This fragment could be divided into three regions with different functions, and structurally it resembled a functional integrative and conjugative element (ICE), ICE*Ec1*, in *Escherichia coli*. The 5′ region of this fragment contained genes similar to a high-pathogenicity island (HPI) of *Yersinia pestis* and *Yersinia pseudotuberculosis*. The middle region was similar to part of a large plasmid in *K. pneumoniae*, and the 3′ region contained genes responsible for DNA conjugative transfer. Therefore, this DNA fragment was designated ICE*Kp1*. Precise excision and extrachromosomal circularization of ICE*Kp1* were detected in *K. pneumoniae* wild-type strain NTUH-K2044. ICE*Kp1* could integrate into the *asn* tRNA loci of the chromosome of another *K. pneumoniae* isolate. The prevalence of ICE*Kp1* was higher in PLA strains (38 of 42 strains) than in non-tissue-invasive strains (5 of 32 strains). Therefore, ICE*Kp1* may contribute to the transmission of the HPI and result in *K. pneumoniae* PLA infection-associated genomic heterogeneity.

Klebsiella pneumoniae, a gram-negative enteric bacterium, is a common pathogen that causes hospital-acquired urinary tract infections, septicemia, and pneumonia, as well as community-acquired pneumonia (1). Recently, community-acquired pyogenic liver abscesses (PLA) caused by *K. pneumoniae* complicated with metastatic meningitis and endophthalmitis have been found globally (13, 15, 19, 21, 25, 27, 37). Capsular serotypes have been reported to play a vital role in the pathogenicity of this organism (18, 20). Using transposon mutagenesis, the *magA* virulence gene has been shown to be associated with mucoviscosity, resistance to serum, and phagocyte killing and virulence in mice (18). Sequencing of the *magA* flanking region (~25 kb) revealed a capsular polysaccharide synthesis (*cps*) region. The region containing *magA* has been shown to be responsible for capsular serotype K1 (17). Genomic heterogeneity is also important in the virulence of *K. pneumoniae* (16, 29). Therefore, both genomic heterogeneity and capsular serotypes play important roles in the pathogenesis of *K. pneumoniae* strains causing liver abscesses.

Horizontal gene transfer contributes substantially to genomic heterogeneity among bacteria. The exchange of DNA plays a critical role in the evolution of bacteria and facilitates the rapid adaptation of bacteria to environmental alterations (24). Horizontal gene transfer is known to be mediated by three mechanisms: transformation, transduction, and conjugation. Pathogenicity islands (PAIs) are defined as 10- to 200-kb DNA fragments that contain gene clusters associated with virulence and are closely related to pathogenic strains. PAIs have G+C contents that are different from the G+C contents of the rest of the whole genome and mobile elements or insertion sequences. Therefore, PAIs are believed to be acquired by horizontal gene transfer. The acquisition of PAIs allows bacteria to grow in and colonize existing niches. However, the mechanism of transmission of PAIs has not been clearly demonstrated yet. Several conjugative and self-transmissible elements that integrate into the bacterial chromosome have been discovered recently (11, 12). These elements had features of plasmids and phages; they could be transferred via conjugation (plasmidlike), and they could integrate into and replicate with the host chromosome (phagelike). Therefore, they were classified as integrative and conjugative elements (ICEs). Because the PAIs were proposed to be transmitted horizontally but no longer appear to be mobile, the progenitors of PAIs might be ICEs.

The high-pathogenicity island (HPI) of *Yersinia* species that carries the yersiniabactin siderophore system is essential for the virulence of *Yersinia* (7, 9, 10). HPI is widely distributed in the family *Enterobacteriaceae* (4, 34, 36), but its mechanism of transmission has not been demonstrated yet. In a recent study, a novel ICE (ICE*Ec1*) of *Escherichia coli* strain ECOR31 was suggested to be a mobilizable progenitor of the HPI (35).

* Corresponding author. Mailing address: Department of Microbiology, National Taiwan University College of Medicine, 1, Sec 1, Jen-Ai Rd., Taipei, Taiwan. Phone: 886-2-23123456, ext. 8292. Fax: 886-2-23948718. E-mail: wangjt@ntu.edu.tw.

▽ Published ahead of print on 2 November 2007.

TABLE 1. Bacterial strains and plasmids used in this study

Strain(s) or plasmid	Description	Reference or source
K. pneumoniae strains		
Clinical isolates	74 isolates collected from National Taiwan University Hospital from 1997 to 2003	18
NTUH-K2044	Clinical strain causing PLA and meningitis	18
MGH78578	ATCC 700721, used for determination of the complete genome sequence at Washington University	ATCC
NTUH-K2044 *int* mutant	NTUH-K2044 isogenic *int* mutant (insertion mutation)	This study
NTUH-K2044 *irp2* mutant	NTUH-K2044 isogenic *irp2* mutant (*irp2* replaced by a kanamycin resistance gene)	This study
NTUH-K2044 *rmpA* mutant	NTUH-K2044 isogenic *rmpA* mutant (mutant 3-20, transposon insertion mutant)	18
NTUH-K2044 *virB1* mutant	NTUH-K2044 isogenic *virB1* mutant (insertion mutation)	This study
NTUH-K2044 *mobB* mutant	NTUH-K2044 isogenic *mobB* mutant (insertion mutation)	This study
N4252 Rif^r	Non-tissue-invasive strain, spontaneous rifampin-resistant mutant	This study
E. coli strains		
HB101	*supE44 hsdS20*(r_B^- m_B^-) *recA13 ara-14 proA2 lacY1 galK2 rpsL20 xyl-5 mtl-1 leuB6 thi-1*	Takara
CC118λ*pir*	Δ(*ara-leu*) *araD* Δ*lacX74 galE galK phoA20 thi-1 rpsE rpoB argE*(Am) *recA1* λ*pir* phage lysogen	23
S17-1λ*pir*	*hsdR recA pro* RP4–2 (Tc::Mu; Km::Tn*7*)(λ*pir*)	31
Plasmids		
pACYC184	Cloning vector, P15A replicon, Cm^r	New England Biolabs
pUT-km	pUTKm1-derived plasmid with mini-Tn*5* excised by EcoRI, *tnp* excised by SalI, and *bla* removed by ApaLI and with insertion of a kanamycin resistance cassette from pUC4K into a PstI site	17

To explore the mechanism of genomic heterogeneity in *K. pneumoniae* strains causing PLA, we compared the complete genome sequences of *K. pneumoniae* strains NTUH-K2044 and MGH78578. A putative ICE containing an HPI was identified in NTUH-K2044 but not in MGH78578, and it was designated ICE*Kp1*. Self-transmission and chromosomal integration were demonstrated in this study.

MATERIALS AND METHODS

Bacterial strains and plasmids. Bacterial strains and plasmids used in this study are listed in Table 1. The 74 clinical isolates were collected from National Taiwan University Hospital from 1997 to 2003 (18, 29). Forty-two of these strains were PLA strains isolated from the blood of patients with PLA with or without meningitis or endophthalmitis complications, and 32 were non-tissue-invasive strains isolated from patients with sepsis but without PLA or other metastatic infections in any tissue. *K. pneumoniae* and *E. coli* were cultured in LB medium supplemented with appropriate antibiotics, including 50 μg/ml kanamycin, 100 μg/ml chloramphenicol, 100 μg/ml streptomycin, and 1,000 μg/ml rifampin.

Sequence analysis. The complete genome sequence of *K. pneumoniae* MGH78578 was determined at Washington University (http://genome.wustl.edu/projects/bacterial/kpneumoniae/). The complete genome sequence of *K. pneumoniae* NTUH-K2044 was determined by collaboration between National Taiwan University College of Medicine and Yangming University in Taiwan (http://genome.nhri.org.tw/kp/index.php). Sequence analysis was performed with Sequencher software (Gene Codes, Wisconsin) and ClustalW (http://www.ebi.ac.uk/Tools/clustalw/index.html). Analysis of homology was performed by comparing sequences with the NCBI BLAST DNA and protein databases.

Construction of *K. pneumoniae* mutant strains. *int*, *virB1*, and *mobB* insertion mutants of *K. pneumoniae* NTUH-K2044 were constructed as previously described (17). Primer pairs (Table 2) were designed to amplify partial regions containing the *int* (int-101F and int-490R), *virB1* (virB1-60F and virB1-359R), and *mobB* (mobB-101F and mobB-500R) genes for mutant construction. The *irp2* deletion mutant was constructed by replacing the *irp2* gene with a kanamycin cassette as previously described (29). The NTUH-K2044 *rmpA* mutant (mutant 3-20) was identified by inverse PCR and sequencing after screening for decreased mucoviscosity by a string test using a mutant library in a previous study (18).

Construction of plasmid pACYC184-*oriT*. Sequences containing *oriT* (nucleotides 65013 to 66772 in the accession number AB298504 sequence after *virB11* and before *mobB*) were amplified from *K. pneumoniae* NTUH-K2044 genomic DNA by PCR using primers oriT-F and oriT-R (Table 2) and cloned into the HincII site of plasmid pACYC184 (Table 1).

Bacterial conjugation. Donors (1×10^8 CFU) and recipients (1×10^8 CFU) grown overnight in 2 ml of 10 mM $MgSO_4$ were mated on a 0.22-μm membrane filter (Advantec, Tokyo, Japan). The membrane was then transferred to Columbia agar plates containing 5% sheep blood and incubated at 37°C overnight. Next, the bacteria were plated on an LB plate supplemented with appropriate antibiotics.

Southern blotting. Approximately 5-μg portions of genomic DNA from various *K. pneumoniae* strains were digested by EcoRV and subjected to Southern hybridization according to manufacturer's instructions (Roche Molecular Biochemicals, Mannheim, Germany). Primers (asn-F and asn-R primers [Table 2]) were designed to generate the digoxigenin-labeled *asn* tRNA gene probe by PCR. A digoxigenin-labeled *int* DNA probe was generated by PCR using primers int-101F and int-490R (Table 2).

Nucleotide sequence accession number. The nucleotide sequence reported in this study has been deposited in the GenBank database under accession number AB298504.

RESULTS

Comparison of the complete genome sequences of *K. pneumoniae* strains. Comparison of the complete genome sequences of *K. pneumoniae* strains NTUH-K2044 and MGH78578 (Table 1) revealed an ~76-kb insertion (accession no. AB298504) in strain NTUH-K2044 (Fig. 1). This DNA fragment was located adjacent to an asparagine (*asn*) tRNA gene and was flanked by 17-bp direct repeats. The average G+C content of the NTUH-K2044 whole genome was ~58%, while the G+C content of this fragment was ~52%. These results suggested that this chromosomal fragment might have been acquired by horizontal transfer. Nucleotide sequence

TABLE 2. Primers used in this study

Primer	Sequence	Purpose	Reference
oriT-F	5′-CAAATAAAATGACAGTCATC-3′	*oriT* cloning	This study
oriT-R	5′-GGCATCGCCCCATCAATT-3′	*oriT* cloning	This study
int-101F	5′-TGGCTCCCGCCACTGGTATC-3′	*int* mutant construction	This study
int-490R	5′-CGGGACGCAACTTCCAGCAG-3′	*int* mutant construction	This study
virB1-60F	5′-GTCCACGGCATTCGACGT-3′	*virB1* mutant construction	This study
virB1-359R	5′-CGGTAGCAGTCTCTGAG-3′	*virB1* mutant construction	This study
mobB-101F	5′-TGCAACAGAAACAACTGGTG-3′	*mobB* mutant construction	This study
mobB-500R	5′-TAATGCAGTGTTTGCGGCAG-3′	*mobB* mutant construction	This study
1	5′-GCACACAGGCATTTTCCAGCAG-3′	Detection of excision	This study
2	5′-AGATGGCTGGATAGGCAC-3′	Detection of excision	This study
3	5′-GACCCAGATACAGATAGC-3′	Detection of excision	This study
4	5′-GGCTGACGTTGCCGACGATAAG-3′	Detection of excision	This study
1′	5′-GGTGACGTTCAAGAGAGACC-3′	Detection of excision	This study
2′	5′-AGAAGGCTTGAGGGTGCGGATT-3′	Detection of excision	This study
3′	5′-GACTCATACCGCTCATGGGCAC-3′	Detection of excision	This study
4′	5′-GTGAATTCATCCTACTGGC-3′	Detection of excision	This study
1166F	5′-GGTGCTCTTTACATCATTGC-3′	*magA* detection	29
500R	5′-GTTCACAACAGCTGCCTGAC-3′	*magA* detection	29
7C4-T71	5′-ATCCTGGAAGCTCACCGTTC-3′	*kfu*/PTS region detection	29
26D6-T32	5′-ATTTCCACGCGGATACCGTC-3′	*kfu*/PTS region detection	29
10E4-2-5F	5′-AGTCGGCCTGGGGTTTAAGG-3′	*allS* region detection	29
10E4-2-475R	5′-CAGTCAACGTGGCGATTCGC-3′	*allS* region detection	29
asn1-F	5′-GTAGACGTGAGAATGGCCTG-3′	ICE integration site analysis	This study
asn1-R	5′-GACAGGCTGTTTTCAGCATC-3′	ICE integration site analysis	This study
asn2-F	5′-CTGGGAGTATGATGCACTGG-3′	ICE integration site analysis	This study
asn2-R	5′-GGTTAATGATCGGCCATTGC-3′	ICE integration site analysis	This study
asn4-F	5′-GTCGCTGTCGTGGACTTTAC-3′	ICE integration site analysis	This study
asn4-R	5′-AGTGATCCTGATGTCGCTGG-3′	ICE integration site analysis	This study
asn3-F	5′-AAGATACGACTCCACACG-3′	ICE integration site analysis	This study
ybtS-R inverse	5′-CGCCCTATTTAATGGTGTAG-3′	ICE integration site analysis	This study
fyuA-F	5′-ATGAAAATGACACGGCT-3′	5′ region prevalence analysis	This study
fyuA-R	5′-TCAGAAGAAATCAATTC-3′	5′ region prevalence analysis	This study
virB1-F	5′-ATGCTTTCCACCACAGC-3′	3′ region prevalence analysis	This study
virB1-R	5′-TTATTCCTCCTCCTCAC-3′	3′ region prevalence analysis	This study
iroN-F	5′-GTCCGGCGGTAACTTCAGCC-3′	Middle region prevalence analysis	This study
iroN-R	5′-TCAGAATGATGCGGTGACAC-3′	Middle region prevalence analysis	This study
HPI 3′-F	5′-CTGCGGTAAATAAATGACG-3′	Connection of 5′ and 3′ regions	This study
virB1-F inverse	5′-GCTGTGGTGGAAAGCAT-3′	Connection of 5′ and 3′ regions	This study
orf3-R	5′-CTTGATGAAAATCTGGTG-3′	Left junction of middle region	This study
orf16-F	5′-AATGTTCTCTGCGCATGG-3′	Right junction of middle region	This study
asn probe-F	5′-CGTTCACACGATTCCTC-3′	*asn* tRNA probe	This study
asn probe-R	5′-GGCTTCTTAAATTTGGCTC-3′	*asn* tRNA probe	This study

analysis of the 76-kb fragment divided it into three functional regions, and this chromosomal fragment was structurally similar to ICE*Ec1* of *E. coli* strain ECOR31 (35). The 5′ region was similar to the HPI of *Yersinia pestis* and *Yersinia pseudotuberculosis*, which is responsible for synthesis of the yersiniabactin siderophore and is closely related to bacterial virulence (7, 9, 10). The production of yersiniabactin in NTUH-K2044 was demonstrated by cross-feeding assays which showed that culture supernatants of NTUH-K2044 promoted the growth of an indicator strain (*Yersinia enterocolitica* strain 5030) under iron-deficient conditions, whereas culture supernatants of the *irp2* mutant did not (22) (data not shown). The middle region was similar to part of the large plasmid in *K. pneumoniae*. The 3′ region resembled genes encoding both a functional mating pair formation system and a DNA-processing region for DNA mobilization in ICE*Ec1* (35). Therefore, this chromosomal fragment was designated ICE*Kp1*.

Sequence analysis of the middle and 3′ regions of ICE*Kp1*. Forty open reading frames (ORFs) larger than 150 nucleotides were identified in the middle and 3′ regions of ICE*Kp1* (Fig. 2 and Table 3).

The middle region (ORF1 to ORF18) contained 12 ORFs (ORF5 to ORF16) that exhibited similarity to part of large plasmid pLVPK in *K. pneumoniae* strain CG43 (14). The *vagC-vagD* operon that was associated with virulence (32) and the *iroN-iroB-iroC-iroD* operon that was responsible for the uptake of a catecholate-type siderophore were also found (5, 6). The function of IroN (the receptor of siderophore) in the middle region was proven by *iroN* transfer to *E. coli* strain H5058, which allowed bacteria to uptake salmochelin siderophores (33) (data not shown). A regulator of the mucoid phenotype (*rmpA*) was also identified in this region (30). The ORFs located in the middle region were related to bacterial virulence, including iron acquisition and mucoviscosity.

The 3′ region contained 22 ORFs (ORF19 to ORF40) that exhibited similarity to the genes responsible for conjugative transfer in ICE*Ec1* of *E. coli* strain ECOR31. Similar to ICE*Ec1* of *E. coli* strain ECOR31, this region also contained

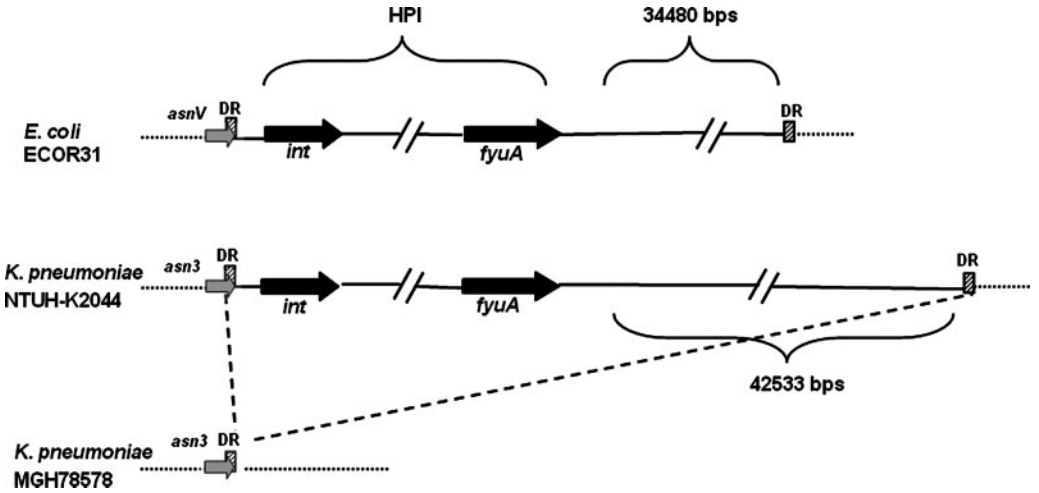

FIG. 1. Seventy-six-kilobase pair insertion in *K. pneumoniae* strain NTUH-K2044. The dashed line indicates that that there was an insertion in *K. pneumoniae* strain NTUH-K2044 compared with strain MGH78578. The insertion was near the asparagine tRNA gene (the *asn* tRNA genes are indicated by gray arrows [*asnV* tRNA gene in *E. coli* ECOR31 and *asn3* tRNA gene in *K. pneumoniae* NTUH-K2044 and MGH78578]). The cross-hatched box indicates the attachment site (*attO*) composed of a 17-bp direct repeat (DR). The black arrows indicate the *int* and *fyuA* genes, which were located in the 5′ and 3′ ends of the HPI. In contrast to the 34,480-bp fragment located adjacent to the HPI core in *E. coli* strain ECOR31, a 42,533-bp fragment was located in the right border of HPI in *K. pneumoniae* strain NTUH-K2044.

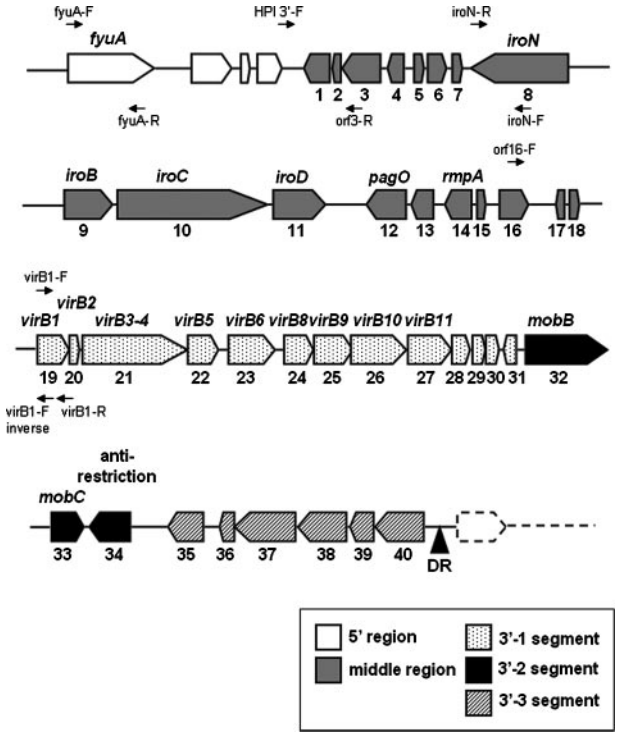

FIG. 2. Genetic alignment of the middle and 3′ regions of ICE*Kp1*. The black triangle indicates the 17-bp direct repeat (DR) and the end of ICE*Kp1*. The large arrows indicate the locations and orientations of ORFs. The ORF numbers and the designations of ORFs are indicated below and above the arrows, respectively. The middle region exhibited similarity to part of large plasmid pLVPK in *K. pneumoniae* strain CG43. The 3′ region contained three functionally distinct segments (segments 3′-1, 3′-2, and 3′-3). The small arrows indicate the locations and orientations of primers used to study the prevalence of ICE*Kp1*.

three functional distinct segments (segments 3′-1, 3′-2, and 3′-3).

Segment 3′-1 (ORF19 to ORF31) contained nine ORFs (ORF19 to ORF27; *virB1* to *virB11*) that were highly similar to region I of ICE*Ec1*. These ORFs were all in the same orientation and might comprise an operon encoding a putative mating pair formation system.

Segment 3′-2 contained three ORFs (ORF32 to ORF34) that were highly similar to region II of ICE*Ec1*. ORF32 to ORF34 (similar to *mobB*, *mobC*, and the anti-restriction protein gene) were associated with mobilization of the conjugative plasmid. Unlike ICE*Ec1*, a putative helicase gene (ORF17) was not found in this segment. A putative origin of transfer (*oriT*), which was located ~140 bp upstream of the *mobB* gene, was also identified. The sequences of *oriT* in ICE*Kp1* had five nucleotide substitutions compared with the sequences in ICE*Ec1* (Fig. 3A). Like the *oriT* sequences of ICE*Ec1*, two inverted repeats and one direct repeat were present in the sequences of ICE*Kp1*. The putative duplicated *nic* site was also found in the second inverted repeat sequence. The ORFs in segment 3′-2 might encode the ability to process the *oriT* sequences and cleave the *nic* site for DNA mobilization.

Segment 3′-3 contained six ORFs (ORF 35 to ORF40) that exhibited similarity to hypothetical genes found in *Nitrobacter hamburgensis*. The sequences in this segment were very different from those in ICE*Ec1*.

Mating pair formation and DNA mobilization of ICE*Kp1*. Five ORFs (*int*, *irp2*, *rmpA*, *virB1*, and *mobB*) were mutated to study the function of ICE*Kp1*. Plasmid pACYC184 carrying cloned *oriT* (plasmid pACYC184-*oriT*) was used to analyze the DNA mobilization ability. *K. pneumoniae* wild-type strain NTUH-K2044 (donor) transformed with plasmid pACYC184 or pACYC184-*oriT* was mated with *E. coli* strain HB101 (recipient). Transconjugants were selected with streptomycin and chloramphenicol to monitor the transfer of plasmid pACYC184 to the

TABLE 3. ORFs in the middle and 3′ regions of ICE*Kp1*

ORF		Product size (amino acids)	Location[a]		Homologous protein(s)	Source	Amino acid identity[b]		Accession no.
No.	Designation		Start site	Stop site			No. of matching amino acids	Total no. of amino acids	
1	ORF1	203	36256	35645	Transposase and inactivated derivatives	*Y. pestis*	179	188	ZP_00797222
2	ORF2	63	36371	36180	IS*100* ORF1	*Shigella dysenteriae*	60	63	ZP_406030
3	ORF3	300	37368	36466	Transposase and inactivated derivatives	*Y. pestis*	297	300	ZP_01175356.1
4	ORF4	126	37936	37556	Hypothetical protein				
5	ORF5	76	38379	38609	VagC	*Salmonella enterica*	71	75	ZP_271744.1
6	ORF6	138	38606	39022	VagD	*K. pneumoniae* CG43	135	138	NP_943352.1
7	ORF7	87	39040	39303	Hypothetical protein LV173	*K. pneumoniae* CG43	51	74	NP_943463.1
8	*iroN*	724	41632	39458	IroN	*E. coli* UTI89	686	725	ZP_540133.1
9	*iroB*	371	42504	43619	IroB	*K. pneumoniae* CG43	362	371	NP_943394.1
10	*iroC*	1231	43706	47401	IroC	*K. pneumoniae* CG43	1198	1214	NP_943393.1
11	*iroD*	409	47507	48736	IroD	*K. pneumoniae* CG43	404	409	NP_943392.1
12	*pagO*	304	50655	49741	PagO	*K. pneumoniae* CG43	275	300	NP_943390.1
13	ORF13	183	51279	50728	Hypothetical protein				
14	*rmpA*	210	52286	51654	Regulator of mucoid phenotype	*K. pneumoniae* CG43	183	210	AAL25252.1
15	ORF15	54	52300	52464	Hypothetical protein				
16	ORF16	217	52828	53481	Hypothetical protein LV256	*K. pneumoniae* CG43	175	179	NP_943388.1
17	ORF17	61	54304	54119	Transposase and inactivated derivatives	*Y. pestis*	61	61	ZP_00797222.1
18	ORF18	77	54789	55022	Putative ATP/GTP-binding protein remnant	*Y. pestis*	46	66	NP_995420
19	*virB1*	236	55095	55805	Pilx1/VirB1-like protein	*E. coli* ECOR31	232	236	AAP70283.1
20	*virB2*	97	55805	56098	VirB2-like protein	*E. coli* ECOR31	97	97	AAP70284.1
21	*virB3-virB 4*	912	56111	58849	Pilx3-4/VirB3-4-like protein	*E. coli* ECOR31	897	912	AAP70302.1
22	*virB5*	234	58867	59571	Pilx5/VirB5-like protein	*E. coli* ECOR31	224	229	AAP70285.1
23	*virB6*	359	59820	60899	Pilx6/VirB6-like protein	*E. coli* ECOR31	296	354	AAP70286.1
24	*virB8*	227	61115	61798	Type IV secretion system VirB8 component	*Y. pestis*	226	227	NP_995427.1
25	*virB9*	302	61795	62703	Type IV secretory pathway VirB9 component	*Y. pestis*	293	301	NP_995428.1
26	*virB10*	416	62747	63997	Pilx10/VirB10-like protein	*E. coli* ECOR31	402	416	AAP70288.1
27	*virB11*	341	63987	65012	Type IV secretory pathway VirB11 component	*Y. pestis*	335	341	NP_995430.1
28	ORF28	132	65009	65407	Hypothetical protein YP_pCRY17	*Yersinia pestis*	118	132	NP_995431.1
29	ORF29	100	65443	65745	YggA-like protein	*E. coli* ECOR31	69	101	AAP70290.1
30	ORF30	101	65788	66093	Unknown	*E. coli* ECOR31	83	101	AAP70307.1
31	ORF31	100	66204	66506	Unknown	*E. coli* ECOR31	99	100	AAP70308.1
32	*mobB*	629	66773	68662	MobB-like protein	*E. coli* ECOR31	607	629	AAP70291.1
33	*mobC*	248	68672	69418	MobC-like protein	*E. coli* ECOR31	212	245	AAP70292.1
34	*ardC*	315	70561	69614	Antirestriction protein	*E. coli* ECOR31	290	315	AAP70295.1
35	ORF35	271	72361	71546	Hypothetical protein				
36	ORF36	115	73009	72662	Hypothetical protein Nham_1368	*N. hamburgensis*	50	93	ZP_576652.1
37	ORF37	464	74403	73009	UBA/THIF-type NAD/flavin adenine dinucleotide binding fold	*N. hamburgensis*	235	459	ZP_576653.1
38	ORF38	375	75503	74376	Hypothetical protein Nham_1370	*N. hamburgensis*	176	353	ZP_576654.1
39	ORF39	182	76146	75598	Conserved hypothetical protein	Gram-negative bacterium	93	175	AAQ10297.1
40	ORF40	367	77292	76189	Hypothetical protein Shewmr7DRAFT_1704	*Shewanella* sp. strain MR-7	147	365	ZP_00855252.1

[a] Nucleotide position in the GenBank accession no. AB298504 sequences.
[b] Determined by BLAST-P analysis.

recipient. *K. pneumoniae* wild-type strains could mediate mobilization of the pACYC184-*oriT* plasmid at a frequency of 4.8×10^{-6} but not mobilization of the pACYC184 plasmid ($<1 \times 10^{-8}$). *int*, *irp2*, and *rmpA* mutant strains were able to transfer plasmid pACYC184-*oriT* (Fig. 3B). *virB1* and *mobB* mutants were not able to mobilize plasmid pACYC184-*oriT* ($<1 \times 10^{-8}$). These results indicated that ICE*Kp1* contains the *virB1* and *mobB* genes responsible for DNA mobilization.

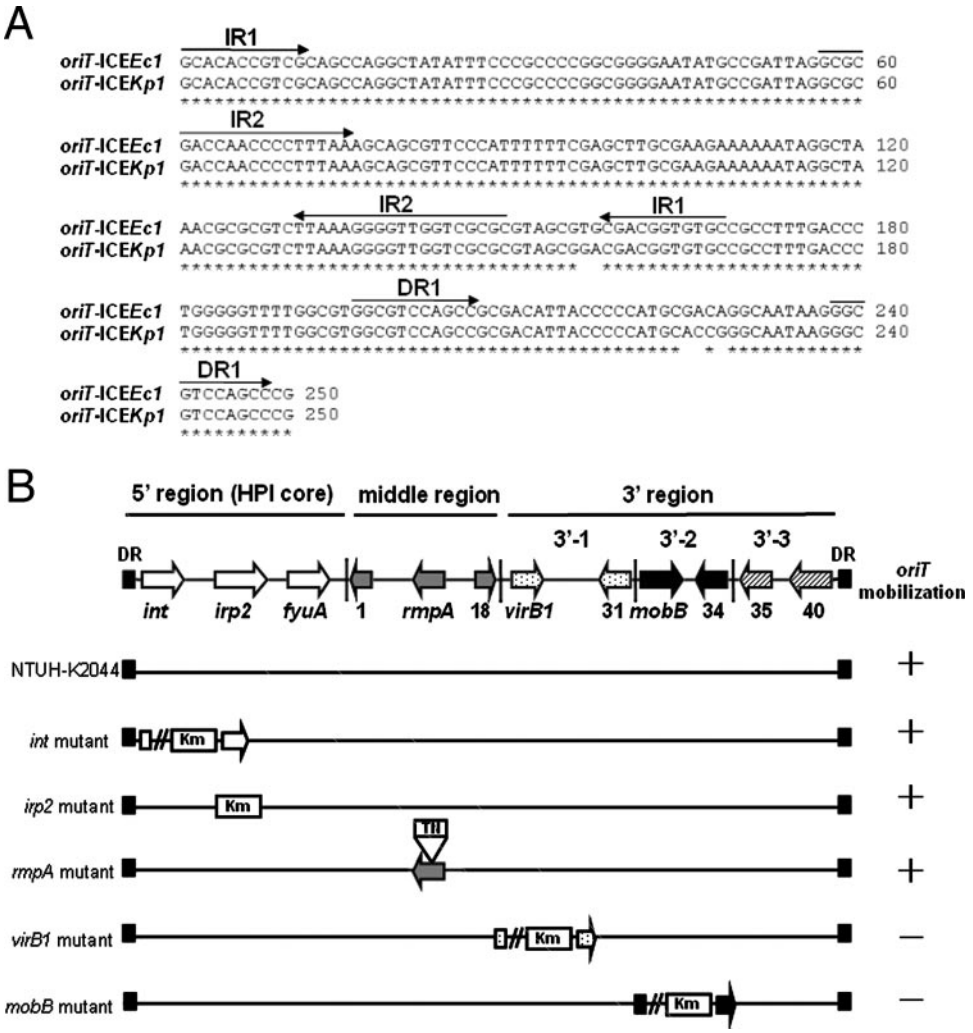

FIG. 3. Functional analysis of ICE*Kp1*. (A) Comparison of *oriT* sequences of ICE*Kp1* and ICE*Ec1*. Asterisks indicate identical nucleotides in the *oriT* sequences of ICE*Kp1* and ICE*Ec1*. The arrows above the sequences indicate the orientations and locations of two inverted repeats (IR1 and IR2) and one direct repeat (DR1). (B) DNA mobilization of ICE*Kp1*. The arrows in the diagram at the top indicate the simplified structure of ICE*Kp1*, which contains three regions. *K. pneumoniae* wild-type strain NTUH-K2044 and mutant strains harboring plasmid pACYC184-*oriT* were mated with *E. coli* strain HB101. A plus sign indicates that the pACYC184-*oriT* plasmid was mobilized to the recipient. A minus sign indicates that mobilization of plasmid pACYC184-*oriT* did not occur. DR, direct repeat.

Precise excision and extrachromosomal circularization of ICE*Kp1*. Generation of circular extrachromosomal intermediates by recombination between the direct repeats at the left and right ICE*Kp1*-chromosome junctions (*attL* and *attR*) was required for dissemination of ICEs (11, 12). A nested PCR assay using primers outside *attL* and *attR* was used to detect whether an extrachromosomal circular ICE*Kp1* was formed (Table 2 and Fig. 4A). Excision and extrachromosomal circularization of ICE*Kp1* in NTUH-K2044 were detected by PCR (Fig. 4B). Sequencing of the PCR products which represented the extrachromosomal and chromosomal junctions confirmed the precise excision and recircularization of ICE*Kp1* in NTUH-K2044 (Fig. 4C). The 17-bp direct repeat identical to the ICE*Ec1* sequence which was the attachment site (*attO*) for recombination was detected in the sequences of both extrachromosomal and chromosomal junctions. Formation of a circular extrachromosomal intermediate was not detected in the NTUH-K2044 *int* mutant (Fig. 4B). Knockout of the other four genes (*irp2*, *rmpA*, *virB1*, and *mobB*) in ICE*Kp1* did not affect the recircularization (Fig. 4B). Therefore, the *int* gene encoding the integrase which catalyzes the recombination reaction was shown to be essential for recircularization of ICE*Kp1*.

Self-transmission of ICE*Kp1*. After the circular extrachromosomal intermediate was detected, whether ICE*Kp1* in *K. pneumoniae* could be transmitted by conjugation was examined. ICE*Kp1*-negative (ICE*Kp1*$^-$) *K. pneumoniae* strain N4252 was used to study the transmission of ICE*Kp1* between *K. pneumoniae* strains. An NTUH-K2044 *rmpA* mutant strain (donor) in which the mobilization of *oriT* and excision of ICE*Kp1* were not affected was mated with spontaneous rifampin-resistant *K. pneumoniae* mutant strain N4252 (recipient). Transconjugants were selected with rifampin and kanamycin to monitor the transfer of ICE*Kp1* to the recipient. The transfer of ICE*Kp1* to the recipient was confirmed by PCR

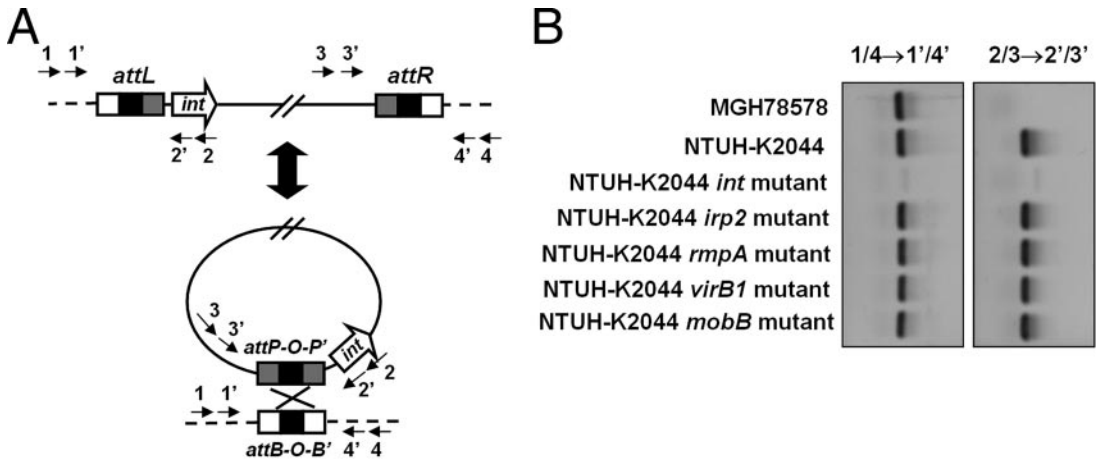

C

Left border	5'-tggttcgagt**CCAGTCAGAGGAGCCAA**ttttctgttt-3'
Chromosome junction (1/4→1'/4')	5'-tggttcgagt**CCAGTCAGAGGAGCCAA**atttaagaag-3'
Extrachromosome junction (2/3→2'/3')	5'-aaaggcgatc**CCAGTCAGAGGAGCCAA**ttttctgttt-3'
Right border	5'-aaaggcgatc**CCAGTCAGAGGAGCCAA**atttaagaag-3'
MGH78578	5'-tggttcgagt**CCAGTCAGAGGAGCCAA**atttaagaag-3'

FIG. 4. Precise excision and extrachromosomal circularization of ICE*Kp1*. (A) Integration and excision model of ICE*Kp1*. The precise excision and extrachromosomal circularization of ICE*Kp1* were mediated by recombination of *attO* sequences (indicated by a black box). Arrows 1, 1′, 2, 2′, 3, 3′, 4, and 4′ represent the primers outside the *attL* and *attR* sequences used to detect the precise excision and extrachromosomal circularization of ICE*Kp1*. (B) Extrachromosomal circular form of ICE*Kp1* detected by nested PCR. PCR using primers 1 and 4 followed by nested PCR using primers 1′ and 4′ detected the *attB* site after excision (left gel). PCR using primers 2 and 3 followed by nested PCR using primers 2′ and 3′ detected the *attP* site in the extrachromosomal circular form (right gel). (C) Sequences of the chromosome and extrachromosomal junctions. Sequences of the chromosomal (1/4→1′/4′) and extrachromosomal (2/3→2′/3′) junctions were compared and aligned with the sequences of the left and right borders of ICE*Kp1* and the sequences without an insertion in MGH78578. The 17-bp direct repeat is indicated by uppercase letters.

(Fig. 5). Donor strain NTUH-K2044 was positive for the *magA*, *kfu*, and *all* genes and ICE*Kp1*. Recipient strain N4252 was negative for the *magA* and *all* genes and ICE*Kp1* but positive for the *kfu* gene (29). The presence of the *magA*, *kfu*, and *all* genes, which were outside ICE*Kp1*, in four randomly selected transconjugants was the same as that in recipient strain N4252. The genes in ICE*Kp1* (such as *int*, *ybtU*, *iroN*, *virB1*, and *mobB*) of the four transconjugants were found to be active for transfer. To further confirm that the transmission of ICE*Kp1* was

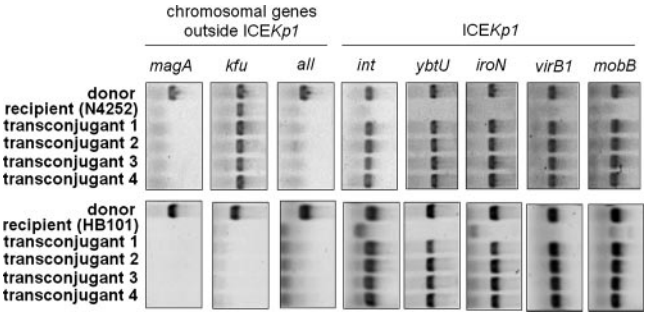

FIG. 5. Self-transmission of ICE*Kp1*. The transfer of ICE*Kp1* from the NTUH-K2044 *rmpA* mutant (donor) to *K. pneumoniae* strain N4252 or *E. coli* strain HB101 (recipient) in four randomly selected transconjugants was analyzed by PCR. Chromosomal genes (*magA*, *kfu*, and *all*) outside ICE*Kp1* were used to differentiate the donor and the recipient. Genes (*int*, *ybtU*, *iroN*, *virB1*, and *mobB*) located in ICE*Kp1* were used to examine the presence of ICE*Kp1*.

recA independent, *recA* mutant *E. coli* strain HB101 was used as the recipient. *rmpA* mutant strain NTUH-K2044 (donor) was mated with *E. coli* strain HB101 (recipient). Transconjugants were selected with streptomycin and kanamycin and then confirmed by PCR (Fig. 5). The absence of the *magA*, *kfu*, and *all* genes, which were outside ICE*Kp1*, and the presence of genes in the ICE*Kp1* of four randomly selected transconjugants revealed that ICE*Kp1* was transferred to *E. coli* strain HB101. The frequencies of ICE*Kp1* transfer from *K. pneumoniae* strain NTUH-K2044 to *K. pneumoniae* strain N4252 or to *E. coli* strain HB101 were similar ($\sim 4 \times 10^{-6}$). In addition, NTUH-K2044 *int*, *virB1*, and *mobB* mutants all failed to transfer ICE*Kp1* to strain N4252 ($< 1 \times 10^{-8}$). These results confirmed that ICE*Kp1* was transferred to the recipient and that the transfer of ICE*Kp1* was *recA* independent. *int*, *virB1*, and *mobB* located in ICE*Kp1* were essential for conjugative transfer of ICE*Kp1*.

Integration site of ICE*Kp1*. ICE*Kp1* was located adjacent to the *asn* tRNA gene. The sequences of the *asn* tRNA gene in *K. pneumoniae* were the same as those in *E. coli*, and the genes have the same attachment site (Fig. 6A). An alignment of four *asn* tRNA genes of *E. coli* and *K. pneumoniae* strains NTUH-K2044 and MGH78578 is shown in Fig. 6A. Compared to *K. pneumoniae* strain NTUH-K2044, an inversion between the *asn2* and *asn4* tRNA genes was found in strain MGH78578. The insertion site of ICE*Kp1* in the four N4252 transconjugants was examined further. Primers flanking the four *asn* tRNA genes and primers derived from the left and right ends

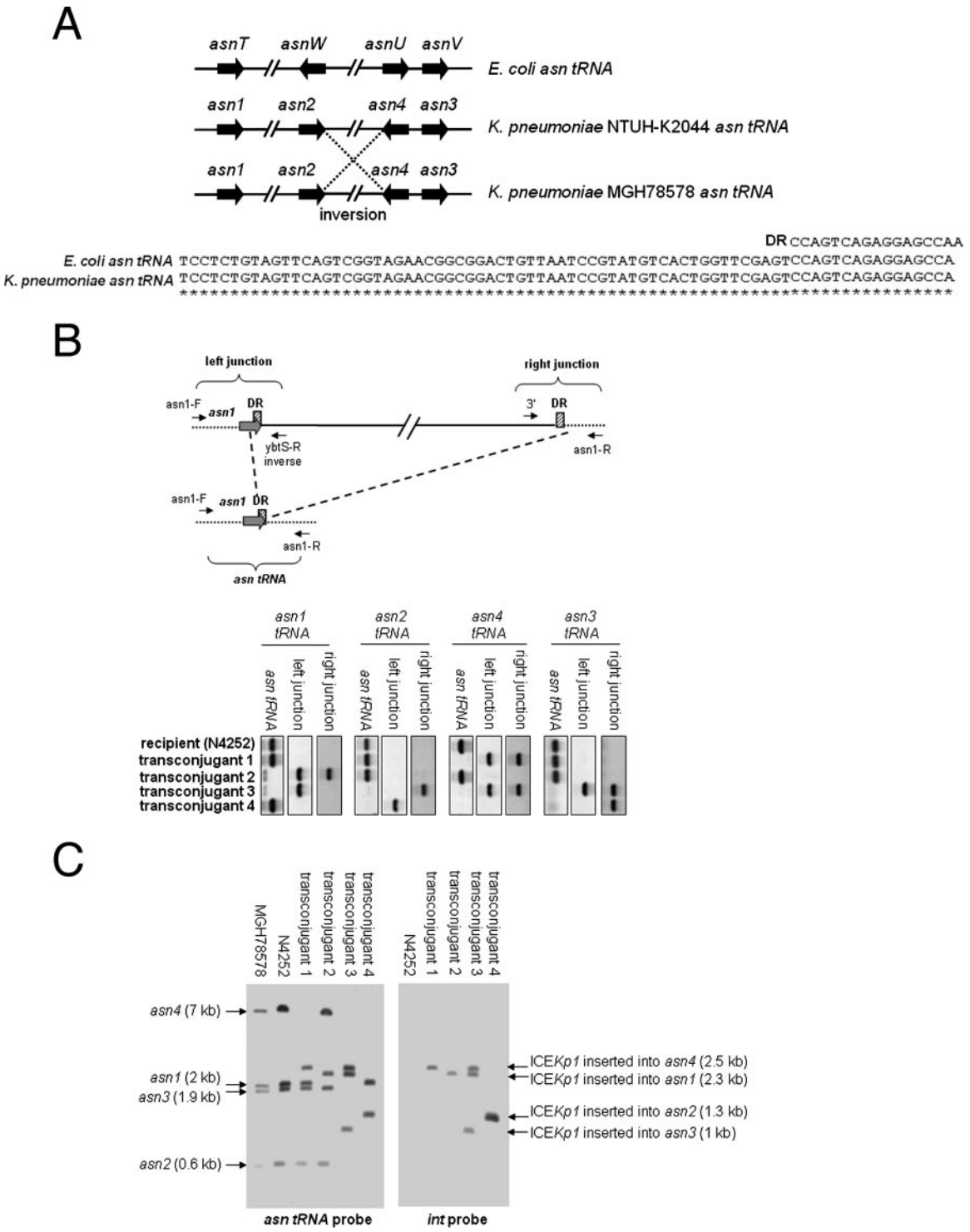

FIG. 6. Integration of ICE*Kp1*. (A) (Top) Alignment of four *asn* tRNA genes of *E. coli* and *K. pneumoniae* strains NTUH-K2044 and MGH78578. The arrows indicate the locations and orientations of *asn* tRNA genes. An inversion between the *asn*2 and *asn*4 tRNA genes was found in strain MGH78578 (indicated by dashed lines). (Bottom) Alignment of sequences of the 17-bp direct repeat (DR) and *asn* tRNA genes of *E. coli* and *K. pneumoniae*. Asterisks indicate identical nucleotides in the *E. coli* and *K. pneumoniae asn* tRNA genes. (B) (Top) Integration of ICE*Kp1* adjacent to *asn* tRNA genes (*asn1* tRNA, for example). The *asn* tRNA is indicated by gray arrows, and the cross-hatched box indicates the 17-bp direct repeat (DR). The small arrows indicate the orientations of primers. The *asn* tRNA gene was detected by primers flanking the *asn1* tRNA gene (asn1-F and asn1-R). The left junction of the ICE*Kp1* insertion was detected by a primer flanking the *asn1* tRNA gene combined with a primer in the left end of ICE*Kp1* (asn1-F and ybtS-R inverse). The right junction of the ICE*Kp1* insertion was detected by a primer flanking the *asn1* tRNA gene combined with a primer in the right end of ICE*Kp1* (asn1-R and 3′). (Bottom) PCR analysis of the integration site of ICE*Kp1* in the four N4252 transconjugants. (C) Southern hybridization of EcoRV-digested DNA from various strains with *asn* tRNA gene (left gel) and *int* (right gel) probes. The arrows indicate the positions of *asn* tRNA gene fragments with or without an ICE*Kp1* insertion.

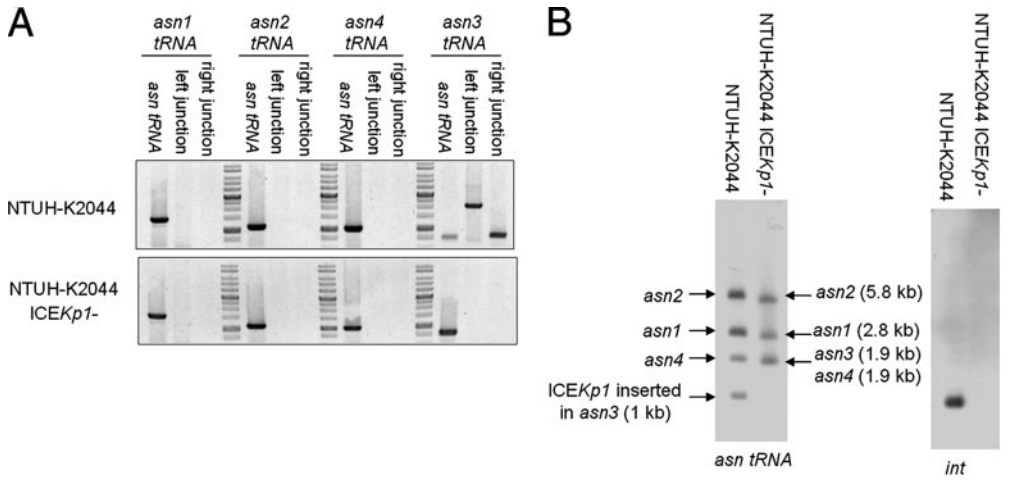

FIG. 7. Mobility of ICE*Kp1* in strain NTUH-K2044. (A) PCR analysis of the location of ICE*Kp1* in strains NTUH-K2044 and NTUH-K2044 ICE*Kp1*$^-$. (B) Southern hybridization of EcoRV-digested DNA from strains NTUH-K2044 and NTUH-K2044 ICE*Kp1*$^-$ with *asn* tRNA gene (left gel) and *int* (right gel) probes. The arrows indicate the positions of *asn* tRNA gene fragments with or without ICE*Kp1* insertion.

of ICE*Kp1* were designed to detect the insertion site of ICE*Kp1* (Table 2 and Fig. 6B). If a 76-kb ICE*Kp1* sequence was inserted into an *asn* tRNA gene, primer pairs flanking the *asn* tRNA gene should not amplify the *asn* tRNA gene; however, the primers flanking the *asn* tRNA gene combined with primers at the left and right ends of ICE*Kp1* should detect the left and right junctions for insertion of ICE*Kp1*. By contrast, if ICE*Kp1* was not inserted into an *asn* tRNA gene, the PCR for detecting the *asn* tRNA gene should remain positive, whereas the PCR for detecting the left and right junctions for the insertion of ICE*Kp1* should be negative. The PCR results showed that ICE*Kp1* was inserted into the *asn4* and *asn1* tRNA genes of transconjugants 1 and 2, respectively (Fig. 6B). Two insertions in the *asn4* and *asn3* tRNA genes of transconjugant 3 were detected. The left junction of another insertion in transconjugant 3 was detected in the *asn1* tRNA gene, whereas the right junction of this insertion was detected in the *asn2* tRNA gene. This insertion might have resulted in a deletion between the *asn1* and *asn2* tRNA genes. In transconjugant 4, the left junction of the ICE*Kp1* insertion was detected in the *asn2* tRNA gene, whereas the right junction was detected in the *asn3* tRNA gene. Similar to what occurred in transconjugant 3, this insertion might have resulted in a deletion between the *asn2* and *asn3* tRNA genes. PCR to determine the genes in the predicted deletion regions in transconjugants 3 and 4 confirmed the occurrence of deletions during the insertion of ICE*Kp1* (data not shown). The integration site of ICE*Kp1* was also confirmed by Southern blotting by hybridization with *asn* tRNA and *int* gene probes (Fig. 6C). The sizes of four *asn* tRNA gene fragments in strain N4252 were same as those in strain MGH78578. The *asn4* tRNA gene fragment (7 kb) was replaced by a 2.5-kb fragment which corresponded to the fragment that encompassed the left border (*int*) of ICE*Kp1* in transconjugant 1. The *asn1* tRNA gene fragment (2 kb) was replaced by a 2.3-kb fragment in transconjugant 2; therefore, the ICE*Kp1* of transconjugant 2 was inserted in the *asn1* tRNA gene. In transconjugant 3, three ICE*Kp1* sequences were inserted in the *asn1*, *asn4*, and *asn3* tRNA genes, and the *asn2* tRNA gene fragment was not present. In transconjugant 4, ICE*Kp1* was inserted in the *asn2* tRNA gene, and the *asn4* and *asn3* tRNA gene fragments were not present. The insertion sites of ICE*Kp1* in four transconjugants analyzed by PCR and Southern blotting were consistent. These results showed that ICE*Kp1* could integrate into all four of the *asn* tRNA gene loci present on the chromosome. There could be more than one ICE*Kp1* insertion into the chromosome, and insertion might result in a deletion between the *asn* tRNA genes.

Mobility of ICE*Kp1* in NTUH-K2044. For the stock culture of strain NTUH-K2044 kept at room temperature, spontaneous loss of the entire ICE*Kp1* sequence was observed in 1 of 300 colonies (NTUH-K2044 ICE*Kp1*$^-$) (Fig. 7A). PCR using primers flanking the four *asn* tRNA genes combined with primers derived from the left and right ends of ICE*Kp1* revealed that the ICE*Kp1* sequence in strain NTUH-K2044 was located adjacent to the *asn3* tRNA gene, and precise excision of ICE*Kp1* was detected (Fig. 7A). A Southern blot hybridized with *asn* tRNA and *int* gene probes revealed that the *asn3* tRNA gene fragment (1.9 kb) was replaced by a 1-kb fragment corresponding to the fragment that encompasses the left border of ICE*Kp1* (Fig. 7B). The results of PCR and Southern blotting confirmed that ICE*Kp1* of strain NTUH-K2044 was inserted into only the *asn3* tRNA and did not mobilize to different *asn* tRNA loci.

Prevalence of ICE*Kp1*in PLA and non-tissue-invasive *K. pneumoniae* strains. The prevalence of ICE*Kp1* in the 42 strains from patients with PLA and the 32 non-tissue-invasive strains was analyzed by PCR using primers for the *fyuA* (5′ region), *iroN* (middle region), and *virB1* (3′ region) genes (Table 2 and Fig. 2). Primers outside the middle region (HPI 3′-F and virB1-F inverse) and primers derived from the left (orf3-R) and right (orf16-F) parts of the middle region were also used (Table 2 and Fig. 2). Seven strains isolated from patients with PLA were positive for *fyuA*, *iroN*, and *virB1*. The presence of the middle region was confirmed by PCR using primers outside the middle region combined with primers derived from the left and right parts of the middle region. Thirty-one PLA strains and five non-tissue-invasive strains were positive for *fyuA* and *virB1* but not for *iroN*. PCR using primers

```
AB298504 35579-35862 TGTCAACGACGGATGAAAAGTGATCCACTTATATCTCCACCAACGGCCCAATATTGATCC 60
AB298504 54053-54336 TGTCAACGACGGATGAAAAGTGATCCACTTATATCTCCACCAACGGCCCAATATTGATCC 60
 pLVPK 193069-193352 TGTCAACGACGGGTAAAAAGTGATCCACTTACATCTCCACCGACGGTCCAATATTGATCC 60
                     ************ * ********** ********* **** ************

AB298504 35579-35862 ACCGTTTTACTCAGGATTAGCTTCTGCTATAATCCCGGCCTTTCGTTTCTGTCTGAGTCG 120
AB298504 54053-54336 ACCGTTTTATTCAGGATTAGCTTCTGCTATAACCCCGGCCTTTCGTTTCTGTCTGAGTCG 120
 pLVPK 193069-193352 ACCGTTTTACTCAGGATTAGCTTCCGCGATAACCCCGGCCTTTCGTTTCTGTTTCAGTCG 120
                     ********* ************** ** **** ****************** * *****

AB298504 35579-35862 ATAGCTTTCTCCTTTGATTTGAACGACATGTGAGTGGTGTAAGATACGGTCCAGCATCGC 180
AB298504 54053-54336 ATAGCTTTCTCCTTTGATTTGAACGACATGTGAGTGGTGTAAGATACGGTCCAGCATCGC 180
 pLVPK 193069-193352 ATAGCTCTCTCCTTTTATTTGAACAACATGTGAGTGGTGTAAGATCCGGTCCAGCATCGC 180
                     ****** ******** ******** ******************** **************

AB298504 35579-35862 TGAGGTCAGTGCTGCATCACCGGCGAACGTTTGATCCCACTGCCCGAACGGCAGATTGGA 240
AB298504 54053-54336 TGAGGTCAGTGCTGCATCACCGGCGAACGTTTGATCCCACTGCCCGAACGGCAGATTGGA 240
 pLVPK 193069-193352 GGATGTCAGCGCCGTATCACCGGCGAACGTCTGATCCCACTGCCCGAACGGCAGGTTGGA 240
                      ** ***** ** * *************** ********************** *****

AB298504 35579-35862 TGTCAGGATCATTGCGCTCTTTTCGTAACGTTTAGCGATGACCT 284
AB298504 54053-54336 TGTCAGGATCATTGCGCTCTTTTCGTAACGTTTAGCGATGACCT 284
 pLVPK 193069-193352 GGTCAGGATCATCGCGCTCTTCTCATAACGTTTGGCGATGACCT 284
                      *********** ******** ** ******** **********
```

FIG. 8. Comparison of sequences from the left and right parts of the middle region and the large plasmid. Asterisks indicate identical nucleotides in nucleotides 35579 to 35862 and 54053 to 54336 in the accession number AB298504 sequence and nucleotides 193069 to 193352 in the pLVPK plasmid sequence.

outside the middle region confirmed the absence of the middle region and the connection of the 5′ and 3′ regions in these strains. Therefore, these strains positive for *fyuA* and *virB1* were suggested to contain ICE*Kp1* but not the middle region. Two non-tissue-invasive strains which were positive for *fyuA* but negative for *iroN* and *virB1* were suggested to contain a small HPI. Therefore, the prevalence of ICE*Kp1* (with or without the middle region) in PLA strains (38 of 42 strains) was higher than the prevalence in the non-tissue-invasive strains (5 of 32 strains). Previous results indicated that 35 of 42 strains from patients with PLA were serotype K1 (*magA*$^+$), whereas 1 of 32 non-tissue-invasive strains was serotype K1 (17). All 36 serotype K1 strains contained this region. Moreover, the nine strains causing PLA with metastatic complications, such as meningitis or endophthalmitis, contained not only the *magA*, *allS*, and *kfu*/PTS (phosphotransferase) regions (29) but also the ICE*Kp1*.

DISCUSSION

Genomic heterogeneity and capsular serotypes both play important roles in the pathogenesis of *K. pneumoniae* causing liver abscesses (16, 18, 29). This study explored the mechanism of genomic heterogeneity by comparing the complete genome sequences of *K. pneumoniae* strains NTUH-K2044 and MGH78578. An approximately 76-kb DNA insertion adjacent to an *asn* tRNA gene was identified in *K. pneumoniae* strain NTUH-K2044. A novel ICE*Ec1* of *E. coli* strain ECOR31 was recently shown to encode a functional mating pair formation system and a DNA-processing system (35). After induction of the integrase, the ICE*Ec1* was shown to excise precisely from the chromosome and recircularize. Based on the similarity of sequences and the genetic structure of ICE*Ec1*, the insertion in *K. pneumoniae* strain NTUH-K2044 was suggested to be an ICE and was designated ICE*Kp1*. Mobilization of *oriT* sequences by ICE*Kp1* and precise excision of ICE*Kp1* were demonstrated. Furthermore, transfer of ICE*Kp1* to another strain was directly demonstrated.

int in ICE*Kp1* was proven to be essential for excision and integration of ICE*Kp1*. Recent studies showed that the HPI excision factor (Hef) and excisionase (Xis_{HPI}) of HPI were also required for the excision and integration of HPI (3, 28). A hypothetical protein composed of 61 amino acids (nucleotides 34091 to 34276 of the accession number AB298504 sequence of ICE*Kp1*) was identical to Hef in *Y. pestis* and *Y. pseudotuberculosis* and was considered to be a Hef homologue that might have similar functions. However, the actual function of this putative Hef protein encoded in ICE*Kp1* needs to be investigated further.

Based on a comparison of sequences with the NCBI BLAST DNA database, the genome of *K. pneumoniae* strain MGH78578 did not have sequences homologous to sequences in ICE*Kp1*. Strain NTUH-K2044 did not have a homologue outside the ICE*Kp1* region either. Integration of ICE*Kp1* resulted from recombination of *attO* sequences present in *asn* tRNA loci of *K. pneumoniae* and not from recombination of other homologous sequences in ICE*Kp1*. ICE*Kp1* contained the HPI (5′ region) and segments (segments 3′-1 and 3′-2) for the formation of the conjugative apparatus and for DNA mobilization which were highly similar to those of ICE*Ec1*. The middle region of ICE*Kp1*, which exhibited similarity to part of large plasmid pLVPK in *K. pneumoniae* strain CG43, was absent in ICE*Ec1*. There were similar 284-bp DNA sequences in the left (nucleotides 35579 to 35862 of the accession number AB298504 sequence) and right (nucleotides 54053 to 54336 of the accession number AB298504 sequence) parts of the middle region (Fig. 8). The 284-bp DNA sequences were also found to be similar to nucleotides 193069 to 193352 of the pLVPK plasmid. The large plasmid of strain NTUH-K2044 also contained these 284-bp DNA sequences (data not shown). These 284-bp DNA sequences flanking the middle region and on the large plasmid might be repeat structures for integration of the

middle region from the large plasmid. However, we did not obtain evidence that ICE*Kp1* is a larger progenitor of ICE*Ec1*. Putative virulence genes, such as the *vagC-vagD* and *iroN-iroB-iroC-iroD* operons and *rmpA*, were found in the middle region of ICE*Kp1* (5, 6, 30, 32). However, the middle region of ICE*Kp1* was detected in only 7 of the 42 strains isolated from patients with PLA. The middle region of ICE*Kp1* was associated with iron acquisition and capsule regulation and could enhance virulence, but it seemed to be not essential for infection. Another difference between ICE*Kp1* and ICE*Ec1* was segment 3′-3. Region III of ICE*Ec1* contained genes either with low homology to chromosomal genes found in *Vibrio cholerae* or with no significant similarity to sequences in the GenBank database. Segment 3′-3 of ICE*Kp1* carried genes which exhibited similarity to the hypothetical genes found in *N. hamburgensis*. These results suggested that these two closely related ICEs might have become diverse during the evolution of bacteria.

The HPI of *Yersinia* species that carries the yersiniabactin siderophore system was essential for the virulence of bacteria (7, 9, 10). The HPI is widely distributed in the family *Enterobacteriaceae* (4, 34, 36), but the mechanism of HPI transfer remains unknown. A recent study suggested that a novel ICE*Ec1* of *E. coli* strain ECOR31 was a mobilizable progenitor of the HPI (35). However, the HPI carried in the ICE was restricted to a single *E. coli* strain, and conjugative transfer of this ICE has not been demonstrated. Another study reported a possible mechanism of HPI dissemination based on site-specific recombination of the excised HPI with the *attB*-presenting RP4 conjugative shuttle plasmid (2). The authors hypothesized that the general model for "trapping" the PAI on a conjugative plasmid bearing an *attB* site could also explain the dissemination of other PAIs. Here we report that an ICE*Kp1* carrying HPI was widely present in *K. pneumoniae* strains causing PLA. The conjugative transfer of ICE*Kp1* to another strain was directly demonstrated in our study, suggesting that it was responsible for the dissemination of HPI in *K. pneumoniae*.

After conjugative transfer of the excised extrachromosomal ICE*Kp1* circular form, the ICE*Kp1* could integrate into any of the four *asn* tRNA loci on the chromosome. As observed for the HPI of *Y. pseudotuberculosis*, the excised form could be found to be inserted in any of the three *asn* tRNA loci present on the chromosome (8). However, ICE*Kp1* in strain NTUH-K2044 did not mobilize to another *asn* tRNA locus, and ICE*Kp1* was more often located adjacent to the *asn3* tRNA gene in our strains (data not shown). PCR and Southern blot analysis of transconjugants revealed that more than one ICE*Kp1* could be inserted into the chromosome (such as transconjugant 3) and that the insertion might result in a deletion between the *asn* tRNA genes (such as transconjugants 3 and 4). These findings implied that the recombination during the integration of ICEs might also facilitate genetic diversity. Most ICEs are thought to be transferred as single-stranded DNA (11, 12). ICEs would be nicked, and single strands of ICEs would be transferred to recipients. After replication, the donor and recipient would each contain a copy of the ICE. Therefore, a copy of ICE*Kp1* was thought to be present in the donor after conjugation. However, we frequently observed spontaneous loss of the entire ICE*Kp1* sequence in our strain. It was difficult to determine whether the donor strain lost or maintained the entire element in the chromosome during transfer of ICE*Kp1*.

In a previous study, 18% of clinical *K. pneumoniae* isolates contained the HPI region (26). ICE*Kp1* carrying HPI was present in many of our clinical *K. pneumoniae* isolates (58%). ICE*Kp1* was more prevalent in PLA strains than in non-tissue-invasive strains. The HPI and *iroN-iroB-iroC-iroD* operon responsible for iron acquisition may increase bacterial growth during infection (5–7). The *rmpA* gene has been shown to be involved in mucoviscosity, which plays an important role in the pathogenesis of bacteria (30). The acquisition of ICE*Kp1* should contribute the pathogenesis of *K. pneumoniae* causing PLA. Serotype K1 has been shown to be the most common serotype in *K. pneumoniae* strains causing PLA (17, 20). A previous pulsed-field gel electrophoresis typing study showed that all of our K1 strains had different clonal origins (13). Our 36 serotype K1 strains all contained the ICE*Kp1* region. Moreover, the nine strains causing PLA with metastatic complications contained not only three virulence-associated regions (*magA*, *allS*, and *kfu*/PTS), as previously described (29), but also the ICE*Kp1* region. The clustering of virulence-associated regions in our strains might indicate that together these regions play an important role in the pathogenesis of this invasive *K. pneumoniae* infection.

ACKNOWLEDGMENTS

This study was supported by grants from the National Science Council, by postdoctoral fellowship PD9503 from the National Health Research Institute, and by a grant from the Liver Disease Prevention and Treatment Research Foundation, Taiwan.

REFERENCES

1. **Abbott, S.** 2003. *Klebsiella*, *Enterobacter*, *Citrobacter*, *Serratia*, *Plesiomonas*, and other *Enterobacteriaceae*, p. 684–700. *In* P. R. Murray, E. J. Baron, J. H. Jorgensen, M. A. Pfaller, and R. H. Yolken (ed.), Manual of clinical microbiology, 8th ed. American Society for Microbiology Press, Washington, DC.
2. **Antonenka, U., C. Nolting, J. Heesemann, and A. Rakin.** 2005. Horizontal transfer of Yersinia high-pathogenicity island by the conjugative RP4 attB target-presenting shuttle plasmid. Mol. Microbiol. **57:**727–734.
3. **Antonenka, U., C. Nolting, J. Heesemann, and A. Rakin.** 2006. Independent acquisition of site-specific recombination factors by asn tRNA gene-targeting genomic islands. Int. J. Med. Microbiol. **296:**341–352.
4. **Bach, S., A. de Almeida, and E. Carniel.** 2000. The Yersinia high-pathogenicity island is present in different members of the family Enterobacteriaceae. FEMS Microbiol. Lett. **183:**289–294.
5. **Baumler, A. J., T. L. Norris, T. Lasco, W. Voight, R. Reissbrodt, W. Rabsch, and F. Heffron.** 1998. IroN, a novel outer membrane siderophore receptor characteristic of *Salmonella enterica*. J. Bacteriol. **180:**1446–1453.
6. **Baumler, A. J., R. M. Tsolis, A. W. van der Velden, I. Stojiljkovic, S. Anic, and F. Heffron.** 1996. Identification of a new iron regulated locus of Salmonella typhi. Gene **183:**207–213.
7. **Bearden, S. W., J. D. Fetherston, and R. D. Perry.** 1997. Genetic organization of the yersiniabactin biosynthetic region and construction of avirulent mutants in *Yersinia pestis*. Infect. Immun. **65:**1659–1668.
8. **Buchrieser, C., R. Brosch, S. Bach, A. Guiyoule, and E. Carniel.** 1998. The high-pathogenicity island of Yersinia pseudotuberculosis can be inserted into any of the three chromosomal asn tRNA genes. Mol. Microbiol. **30:**965–978.
9. **Buchrieser, C., M. Prentice, and E. Carniel.** 1998. The 102-kilobase unstable region of *Yersinia pestis* comprises a high-pathogenicity island linked to a pigmentation segment which undergoes internal rearrangement. J. Bacteriol. **180:**2321–2329.
10. **Buchrieser, C., C. Rusniok, L. Frangeul, E. Couve, A. Billault, F. Kunst, E. Carniel, and P. Glaser.** 1999. The 102-kilobase *pgm* locus of *Yersinia pestis*: sequence analysis and comparison of selected regions among different *Yersinia pestis* and *Yersinia pseudotuberculosis* strains. Infect. Immun. **67:**4851–4861.
11. **Burrus, V., G. Pavlovic, B. Decaris, and G. Guedon.** 2002. Conjugative transposons: the tip of the iceberg. Mol. Microbiol. **46:**601–610.
12. **Burrus, V., and M. K. Waldor.** 2004. Shaping bacterial genomes with integrative and conjugative elements. Res. Microbiol. **155:**376–386.
13. **Chang, S. C., C. T. Fang, P. R. Hsueh, Y. C. Chen, and K. T. Luh.** 2000.

Klebsiella pneumoniae isolates causing liver abscess in Taiwan. Diagn. Microbiol. Infect. Dis. **37:**279–284.
14. **Chen, Y. T., H. Y. Chang, Y. C. Lai, C. C. Pan, S. F. Tsai, and H. L. Peng.** 2004. Sequencing and analysis of the large virulence plasmid pLVPK of Klebsiella pneumoniae CG43. Gene **337:**189–198.
15. **Chiu, C. T., D. Y. Lin, and Y. F. Liaw.** 1988. Metastatic septic endophthalmitis in pyogenic liver abscess. J. Clin. Gastroenterol. **10:**524–527.
16. **Chou, H. C., C. Z. Lee, L. C. Ma, C. T. Fang, S. C. Chang, and J. T. Wang.** 2004. Isolation of a chromosomal region of *Klebsiella pneumoniae* associated with allantoin metabolism and liver infection. Infect. Immun. **72:**3783–3792.
17. **Chuang, Y. P., C. T. Fang, S. Y. Lai, S. C. Chang, and J. T. Wang.** 2006. Genetic determinants of capsular serotype K1 of Klebsiella pneumoniae causing primary pyogenic liver abscess. J. Infect. Dis. **193:**645–654.
18. **Fang, C. T., Y. P. Chuang, C. T. Shun, S. C. Chang, and J. T. Wang.** 2004. A novel virulence gene in Klebsiella pneumoniae strains causing primary liver abscess and septic metastatic complications. J. Exp. Med. **199:**697–705.
19. **Fang, F. C., N. Sandler, and S. J. Libby.** 2005. Liver abscess caused by *magA*$^+$ *Klebsiella pneumoniae* in North America. J. Clin. Microbiol. **43:**991–992.
20. **Fung, C. P., F. Y. Chang, S. C. Lee, B. S. Hu, B. I. Kuo, C. Y. Liu, M. Ho, and L. K. Siu.** 2002. A global emerging disease of Klebsiella pneumoniae liver abscess: is serotype K1 an important factor for complicated endophthalmitis? Gut **50:**420–424.
21. **Golia, P., and M. Sadler.** 2006. Pyogenic liver abscess: Klebsiella as an emerging pathogen. Emerg. Radiol. **13:**87–88.
22. **Haag, H., K. Hantke, H. Drechsel, I. Stojiljkovic, G. Jung, and H. Zahner.** 1993. Purification of yersiniabactin: a siderophore and possible virulence factor of Yersinia enterocolitica. J. Gen. Microbiol. **139:**2159–2165.
23. **Herrero, M., V. de Lorenzo, and K. N. Timmis.** 1990. Transposon vectors containing non-antibiotic resistance selection markers for cloning and stable chromosomal insertion of foreign genes in gram-negative bacteria. J. Bacteriol. **172:**6557–6567.
24. **Jain, R., M. C. Rivera, J. E. Moore, and J. A. Lake.** 2002. Horizontal gene transfer in microbial genome evolution. Theor. Popul. Biol. **61:**489–495.
25. **Ko, W. C., D. L. Paterson, A. J. Sagnimeni, D. S. Hansen, A. Von Gottberg, S. Mohapatra, J. M. Casellas, H. Goossens, L. Mulazimoglu, G. Trenholme, K. P. Klugman, J. G. McCormack, and V. L. Yu.** 2002. Community-acquired Klebsiella pneumoniae bacteremia: global differences in clinical patterns. Emerg. Infect. Dis. **8:**160–166.
26. **Koczura, R., and A. Kaznowski.** 2003. Occurrence of the Yersinia high-pathogenicity island and iron uptake systems in clinical isolates of Klebsiella pneumoniae. Microb. Pathog. **35:**197–202.
27. **Lederman, E. R., and N. F. Crum.** 2005. Pyogenic liver abscess with a focus on Klebsiella pneumoniae as a primary pathogen: an emerging disease with unique clinical characteristics. Am. J. Gastroenterol. **100:**322–331.
28. **Lesic, B., S. Bach, J. M. Ghigo, U. Dobrindt, J. Hacker, and E. Carniel.** 2004. Excision of the high-pathogenicity island of Yersinia pseudotuberculosis requires the combined actions of its cognate integrase and Hef, a new recombination directionality factor. Mol. Microbiol. **52:**1337–1348.
29. **Ma, L. C., C. T. Fang, C. Z. Lee, C. T. Shun, and J. T. Wang.** 2005. Genomic heterogeneity in Klebsiella pneumoniae strains is associated with primary pyogenic liver abscess and metastatic infection. J. Infect. Dis. **192:**117–128.
30. **Nassif, X., N. Honore, T. Vasselon, S. T. Cole, and P. J. Sansonetti.** 1989. Positive control of colanic acid synthesis in Escherichia coli by rmpA and rmpB, two virulence-plasmid genes of Klebsiella pneumoniae. Mol. Microbiol. **3:**1349–1359.
31. **Parke, D.** 1990. Construction of mobilizable vectors derived from plasmids RP4, pUC18 and pUC19. Gene **93:**135–137.
32. **Pullinger, G. D., and A. J. Lax.** 1992. A Salmonella dublin virulence plasmid locus that affects bacterial growth under nutrient-limited conditions. Mol. Microbiol. **6:**1631–1643.
33. **Reissbrodt, R., and W. Rabsch.** 1988. Further differentiation of Enterobacteriaceae by means of siderophore-pattern analysis. Zentralbl. Bakteriol. Mikrobiol. Hyg. Ser. A **268:**306–317.
34. **Schubert, S., S. Cuenca, D. Fischer, and J. Heesemann.** 2000. High-pathogenicity island of Yersinia pestis in Enterobacteriaceae isolated from blood cultures and urine samples: prevalence and functional expression. J. Infect. Dis. **182:**1268–1271.
35. **Schubert, S., S. Dufke, J. Sorsa, and J. Heesemann.** 2004. A novel integrative and conjugative element (ICE) of Escherichia coli: the putative progenitor of the Yersinia high-pathogenicity island. Mol. Microbiol. **51:**837–848.
36. **Schubert, S., A. Rakin, H. Karch, E. Carniel, and J. Heesemann.** 1998. Prevalence of the "high-pathogenicity island" of *Yersinia* species among *Escherichia coli* strains that are pathogenic to humans. Infect. Immun. **66:**480–485.
37. **Wang, J. H., Y. C. Liu, S. S. Lee, M. Y. Yen, Y. S. Chen, J. H. Wang, S. R. Wann, and H. H. Lin.** 1998. Primary liver abscess due to Klebsiella pneumoniae in Taiwan. Clin. Infect. Dis. **26:**1434–1438.